

Bioinspired, Spine-Like, Flexible, Rechargeable Lithium-Ion Batteries with High Energy Density

Guoyu Qian, Bin Zhu, Xiangbiao Liao, Haowei Zhai, Arvind Srinivasan, Nathan Joseph Fritz, Qian Cheng, Mingqiang Ning, Boyu Qie, Yi Li, Songliu Yuan, Jia Zhu, Xi Chen, and Yuan Yang*

The rapid development of flexible and wearable electronics proposes the persistent requirements of high-performance flexible batteries. Much progress has been achieved recently, but how to obtain remarkable flexibility and high energy density simultaneously remains a great challenge. Here, a facile and scalable approach to fabricate spine-like flexible lithium-ion batteries is reported. A thick, rigid segment to store energy through winding the electrodes corresponds to the vertebra of animals, while a thin, unwound, and flexible part acts as marrow to interconnect all vertebra-like stacks together, providing excellent flexibility for the whole battery. As the volume of the rigid electrode part is significantly larger than the flexible interconnection, the energy density of such a flexible battery can be over 85% of that in conventional packing. A nonoptimized flexible cell with an energy density of 242 Wh L⁻¹ is demonstrated with packaging considered, which is 86.1% of a standard prismatic cell using the same components. The cell also successfully survives a harsh dynamic mechanical load test due to this rational bioinspired design. Mechanical simulation results uncover the underlying mechanism: the maximum strain in the reported design ($\approx 0.08\%$) is markedly smaller than traditional stacked cells ($\approx 1.1\%$). This new approach offers great promise for applications in flexible devices.

crucial.^[11–20] However, it is difficult to obtain good flexibility and high energy density in batteries concurrently.^[21–23] In the past decades, considerable efforts have been made to improve the flexibility of lithium (Li)-ion batteries without sacrificing their performance.^[24–27] For example, single-layer and ultrathin batteries have been reported with excellent flexibility, however, the energy density is largely compromised, especially when packaging is considered.^[28] Wire-shaped batteries have attracted much attention recently because of the easiness to be twisted, tied, and woven into fabrics, but the low mass loading of active electrode materials limits their energy density.^[21,26,29,30] To increase the energy density of flexible batteries, the piling up or combination of small size cell units in series has been proposed to enable them flexible via the gap between different units.^[31] However, the complexity in assembling these microbatteries not only increases cost, but also reduces stability

and consistency, which limits its application. The scalable fabrication of Li-ion batteries with high energy density and excellent mechanical properties/flexibility simultaneously remains a big challenge.

Flexible electronics have great promise for wide applications including communication,^[1–3] healthcare,^[4,5] and sensors.^[6–10] As an efficient power source for these flexible electronics, the development of flexible batteries with high performance is

and consistency, which limits its application. The scalable fabrication of Li-ion batteries with high energy density and excellent mechanical properties/flexibility simultaneously remains a big challenge.

G. Y. Qian, B. Zhu, H. W. Zhai, N. J. Fritz, Dr. Q. Cheng, M. Q. Ning, B. Y. Qie, Prof. Y. Yang
Program of Materials Science and Engineering
Department of Applied Physics and Applied Mathematics
Columbia University
New York, NY 10025, USA
E-mail: yy2664@columbia.edu

G. Y. Qian, Prof. S. L. Yuan
School of Physics
Huazhong University of Science and Technology
Wuhan 430074, P. R. China

B. Zhu, Prof. J. Zhu
College of Engineering and Applied Science
Nanjing University
Nanjing 210093, P. R. China

X. B. Liao, Prof. X. Chen
Department of Earth and Environmental Engineering
Columbia University
New York, NY 10025, USA

A. Srinivasan
Department of Mechanical Engineering
Columbia University
New York, NY 10025, USA

Y. Li
Visual Communication Department
School of the Art Institute of Chicago
Chicago, IL 60603, USA

 The ORCID identification number(s) for the author(s) of this article can be found under <https://doi.org/10.1002/adma.201704947>.

DOI: 10.1002/adma.201704947

The animal spine is mechanically robust, highly flexible, and distortable, as they contain soft marrow components to interconnect hard vertebra parts. Herein, inspired by the structure of spine, we demonstrate a scalable approach to fabricate flexible Li-ion batteries with high energy density (Figure 1a). As shown in Figure 1b, the conventional anode/separator/cathode/separator stack is cut into a long strip with multiple branches extending out in the perpendicular direction. Then the strip in each branch is wrapped around the backbone to form thick stacks for storing energy, which corresponds to the vertebra in the spine. The unwound part interconnects all vertebra-like thick stacks together, which functions in a similar way as the soft marrow, providing excellent flexibility for the whole device. With such an integrated design, the cell energy density is only limited by the longitudinal percentage of vertebra-like stacks compared to the whole length, which can be easily over 90%. Therefore, such battery can have a high energy density >85% of conventional prismatic cell, with extra redundancy considered. Here, an unoptimized LiCoO₂/graphite spine-like flexible cell is fabricated with energy density of 242 Wh L⁻¹ including the package, which exhibits 86.1% of its prismatic cell counterpart with the same mass loading and packaging (see Supporting Information for more details). A stable cycling of over 100 cycles with initial discharge capacity of 151 mA h g⁻¹ and retention of 94.3% is achieved, even with various kinds of mechanical deformation applied. The cell also survives a continuous dynamic mechanical load test, which was rarely reported in previous literature. At 0.5 C, the discharge capacity remains above 125 mA h g⁻¹ (1.59 mA h cm⁻²) steadily under continuous dynamic load. In addition to experiments, numerical mechanical simulation is also carried out, which further uncovered the underlying mechanism of the excellent stability in our design. The largest strain on the interconnected joints is only 0.08%, which is much smaller than that in

prismatic cell (1.8%) and stacked pouch cell (1.1%). Therefore, our spine-like design is much more mechanically robust compared to conventional designs. We anticipate that this bio-inspired, scalable method to fabricate flexible battery could open new opportunities for the commercialization of flexible devices.

To evaluate the electromechanical performance of the spine-like battery in different stress environments, a LiCoO₂/graphite full cell was deformed from flat to flexed and twisted during cycling at 0.2 C (28 mA g⁻¹), and the discharge capacity remained over 94.3% after 100 cycles with a stable Coulombic efficiency above 99.9% (Figure 2a). The battery was first cycled in a flat configuration (region I) for 50 cycles, and capacity decays slowly from 151.4 to 144.8 mA h g⁻¹ (0.087% decay per cycle). Then the cell was flexed 10 000 times into the bent configuration with a bending diameter of 20 mm (I/II boundary) as Figure S3 in the Supporting Information shows, then cycled in static flexed configuration (region II). Clearly the bending does not affect the cell's performance. The discharge capacity immediately after flexing is 146.5 mA h g⁻¹, and remains at 145.7 mA h g⁻¹ after 20 cycles, corresponding to only 0.027% loss per cycle. Then the cell was returned to the relaxed configuration with a steady cycling (region III). Subsequently, the battery was subjected to 1000 torsional deformations of 90° (III/IV boundary) followed by cycling at the static twisted state (Figure 2b). Again, no apparent decay was observed for ten cycles (region IV). The capacity fading rate in the twisted state is only 0.046% per cycle. As the last step, the cell is returned to the relaxed configuration with a steady cycling (region V). Such excellent cycling performance demonstrates that static deformation has no effect on the cycling performance of as-designed spine-like batteries. The increase of capacity in the initial three cycles was likely to be a result of electrolyte infiltration (Figure 2a).

Besides stable capacity upon cycling, the as-constructed flexible battery also shows stable voltage profile no matter if

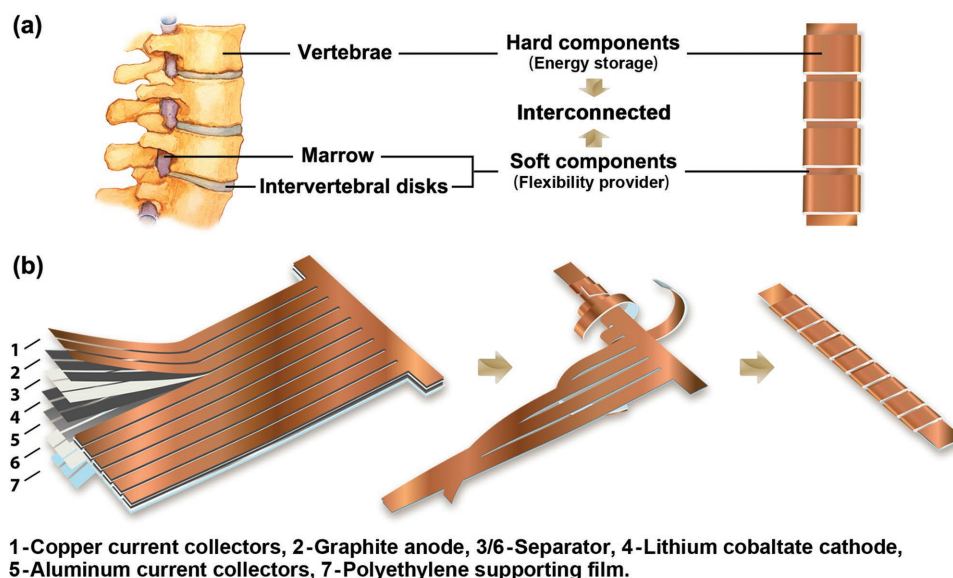


Figure 1. The schematic of the structure and the fabrication process of a spine-like battery. a) Schematic illustration of bioinspired design, the vertebrae corresponds to thick stacks of electrodes and soft marrow corresponds to unwound part interconnects all the stacks. b) The process to fabricate the spine-like battery, multilayers of electrodes were first cut into designed shape, then strips extending out were wound around the backbone to form spine-like structure.

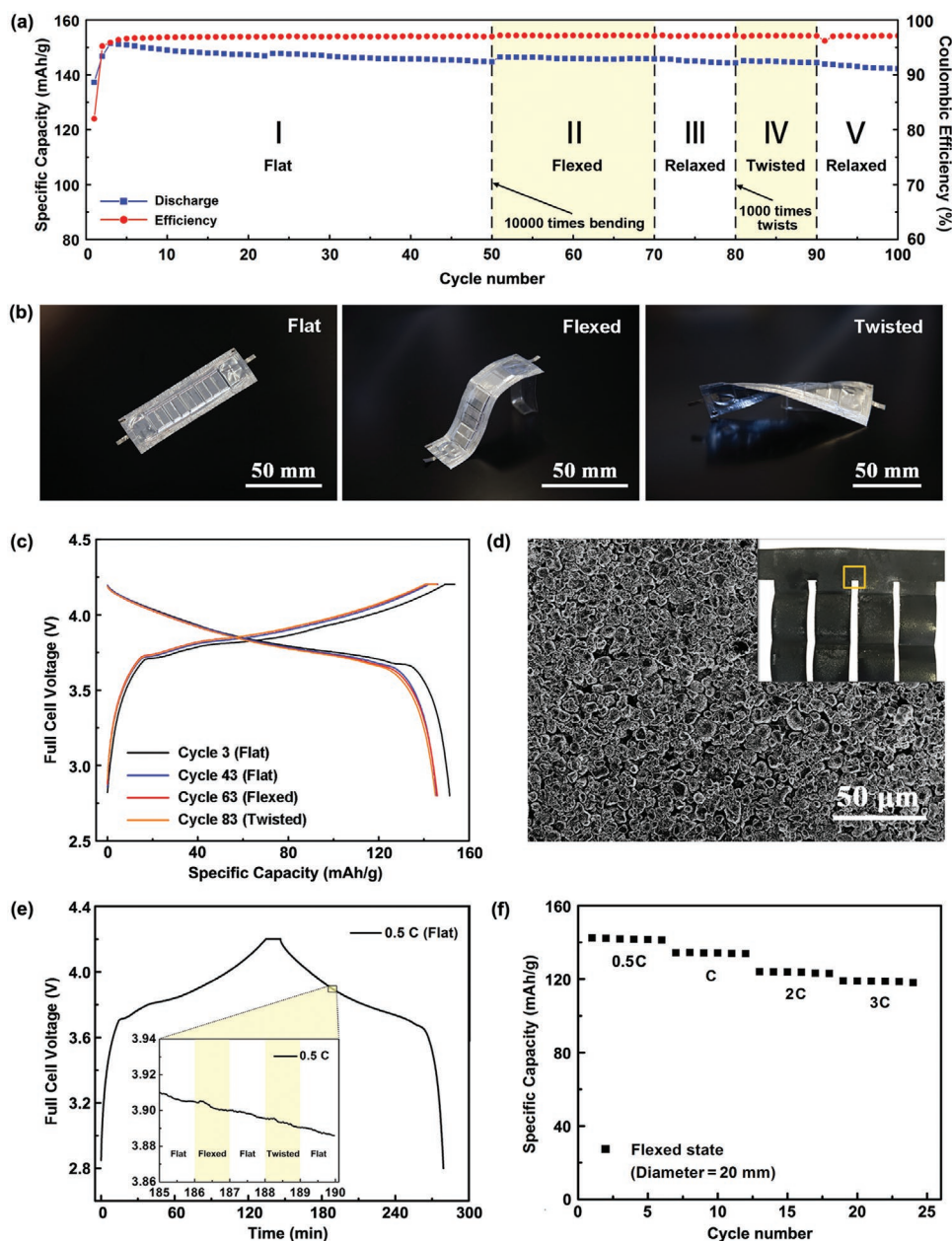


Figure 2. The electrochemical performance of the spine-like battery in different stress conditions. a) Charge/discharge cycling test of the spine-like battery in different configurations at 0.2 C (28 mA g^{-1}). b) Optical images of the spine battery in the state of flat, flexed, and twisted. c) Galvanostatic charge–discharge curves for the 3rd, 43th, 63th, and 83th cycles of the battery in different conditions. d) Scanning electron microscopy (SEM) images of a LiCoO_2 cathode at the boundary of wound/unwound part (yellow line part of the optical image inset) after 100 electrochemical cycles. This region undergoes largest strain during bending. e) The galvanostatic charge–discharge curve at the rate of 0.5 C in which the battery was continuously flexed or twisted (the inset presents the voltage profile under continuous mechanical deformation (flat, flexed, and twisted) of the battery at 0.5 Hz). f) Rate performance of the spine-like battery in which the current densities ranged from 0.5 to 3 C in the static flexed configuration.

it is flexed or twisted, as illustrated in Figure 2c. No apparent increase in overpotential is observed. Compared with noticeable reports in the literature (Table 1),^[25,26,28,32,33] this is the first time a flexible battery has been reported with such high stability with respect to a small bending diameter of 20 mm and a torsion angle of 90° , to the best of our knowledge. After cycling, the battery is disassembled to examine the morphology change of electrode materials. Compared to a pristine electrode (Figure S4,

Supporting Information), it was found that the LiCoO_2 (LCO) electrode remained intact with no obvious cracking or peeling from the aluminum foil (Figure 2d), confirming the mechanical stability of our design. To further illustrate the flexibility of our design, the cell was continuously flexed or twisted during discharge, with a current of 0.5 C (70 mA g^{-1}) applied at a frequency of 0.5 Hz. The level of bending and twisting was the same as those in Figure 2b. As shown in Figure 2e, neither

Table 1. The comparison of electrochemical performance with literature reports on flexible batteries.

Type of flexibility	Electrode materials	Specific capacity		Energy density [Wh L ⁻¹]	Capacity decay (per ten cycles)	Coulombic efficiency (after stabilization)	Ref.
		Gravimetric [mA h g ⁻¹]	Volumetric [mA h cm ⁻³]				
Bendable	LiCoO ₂ /Li ₄ Ti ₅ O ₁₂	128	3.30	7.59	7.7%	93.0%	[25]
Bendable	Ag/Zn		52.3	78.4	0.6%	99.0%	[26]
Bendable	LiCoO ₂ /Li		0.579	2.20	0.9%	99.8%	[28]
Bendable/ twistable	LiCoO ₂ /Li ₄ Ti ₅ O ₁₂	85.5	29.0	69.6	5.3%	99.8%	[32]
Bendable	LiMn ₂ O ₄ /Li	110	7.33	19.1	1.8%	98.5%	[33]
Bendable/twistable	LiCoO ₂ /Graphite	151	63.9	242	0.6%	99.9%	Our work

bending nor twisting interrupted the voltage curve, and the fluctuation was smaller than 3 mV, indicating a change of impedance less than 0.18 Ω, much less than the pristine cell (Figure S5, Supporting Information). The voltage profile is stable even when the cell was continuously flexed and twisted during the whole discharge (Figure S6, Supporting Information). The battery in the flexed state (bending diameter $D = 20$ mm) was also cycled at higher current densities, and the capacity retention reached 95.1%, 87.8%, and 84.3% of that at 0.5 C for 1, 2, and 3 C, respectively, demonstrating appealing power capability for commercial applications.

As multiple-layer thick electrodes can be used in such spine-like cell, high energy density close to commercial cells can be achieved. The energy density of our unoptimized cell is 242 Wh L⁻¹ with packaging included. Such value is 86% of the theoretical energy density based on components with the same thickness and material loading. The specific energy of the spine-like cell also reaches 96 Wh kg⁻¹ with packaging included. The lower values compared with commercial Li-ion cells mainly arise from thicker metal substrate, less mass loading (1.8 vs 3–4 mA h cm⁻²), single-side electrode coating instead of two sides, and heavier packaging. With further optimization, we are confident to reach energy density and specific energy ≈85% of commercial Li-ion batteries.

Flexible batteries for wearable applications are likely to undergo thousands of flexed cycles throughout their lifetime, so mechanical endurance under repetitive mechanical load is a basic requirement for practical applications, which is also a key challenge for flexible batteries. Therefore, a dynamic mechanical load experiment was performed to demonstrate the mechanical endurance of our spine-like flexible battery. In the experiment, the two ends of battery were bound onto two actuators. One actuator was fixed while the other moved at a speed of 3 mm s⁻¹ and traveled a distance of 30 mm. Thus, the flexible cell shuttled between the flat state and the flexed state with a bending diameter of 20 mm with a frequency of once per 30 s (Figure 3a; Video S1, Supporting Information). The optical images in Figure 3b present the battery at different stages in the experiment. When cycled at 0.5 C, it is obvious that the battery can still be continuously charged/discharged during such deformation (Figure 3c, cycles 6–15; Video S2 in the Supporting Information). At the start of continuous bending, the discharge capacity is 129.5 mA h g⁻¹ (cycle 6), after a slight decrease of 3.8 mA h g⁻¹ from cycles 6–10, the specific discharge capacity is maintained steadily from 125.7 mA h g⁻¹ in

the 10th cycle to 124.6 mA h g⁻¹ in the 15th cycle. Regarding to voltage profile, when the cell underwent dynamic flexing, the average discharge voltage decreased by 83 mV and the average charge voltage increased by 88.8 mV, compared to the flat state (cycle 8 vs cycle 3, Figure 3d). This indicates that the system adjusted itself to accommodate strain in continuous bending in the first several cycles (cycle 8 vs cycle 3). However, once several cycles are done under continuous bending, no further degradation in voltage profile was observed, no matter whether the cell is bent or flat (cycle 8 vs cycle 18). Such stability under dynamic bending suggests that at least most active electrode materials did not lose contact with the current collectors in this process. In comparison, we also tested the electrochemical performance of prismatic and stacked cell with the same size in the dynamic flexing configuration, as shown in Figure 3e and Figure S12 (Supporting Information), respectively. The voltage curves of prismatic and stacked cells exhibit tremendous drop (≈0.5 V) because of unstable contacts between electrode and current collector during the dynamic flexing.

To further demonstrate its practical applications, a fully charged spine-like battery with a weight of 4.86 g and capacity of 123.53 mA h was used to power a light-emitting diode (LED) light and a smart watch (Figure 4a,b; Videos S3,S4, Supporting Information). The LED and watch maintained good functionality even when the battery was flexed and twisted, suggesting our design is compatible with commercial needs in flexible electronics.

To understand the excellent flexibility of our design, mechanical analysis was carried out. Qualitatively, the spine-like structure consisting of thick stacks and thin interconnect elements suggests very low effective bending stiffness (Figure 5a), and we analytically evaluated its effective bending stiffness by calculating the spring constant per unit width k of the whole battery as a cantilever (details in the Supporting Information). A smaller k indicates higher flexibility. Figure 5b shows that k/k_0 decreases exponentially with increasing length fraction x of the marrow-like thin interconnects, where k_0 is the bending stiffness of thick electrode stacks (vertebra part). Thus, even a small x (e.g., ≈0.1) can allow high flexibility of the spine-like structure, compared with stacked or prismatic structures (morphology shown in Figure S7 in the Supporting Information). Meanwhile, such small x sacrifices little on energy density at the cell level. To further compare the flexibility of our spine-like structure over the other two conventional designs, we quantified the strain distributions of the three structures

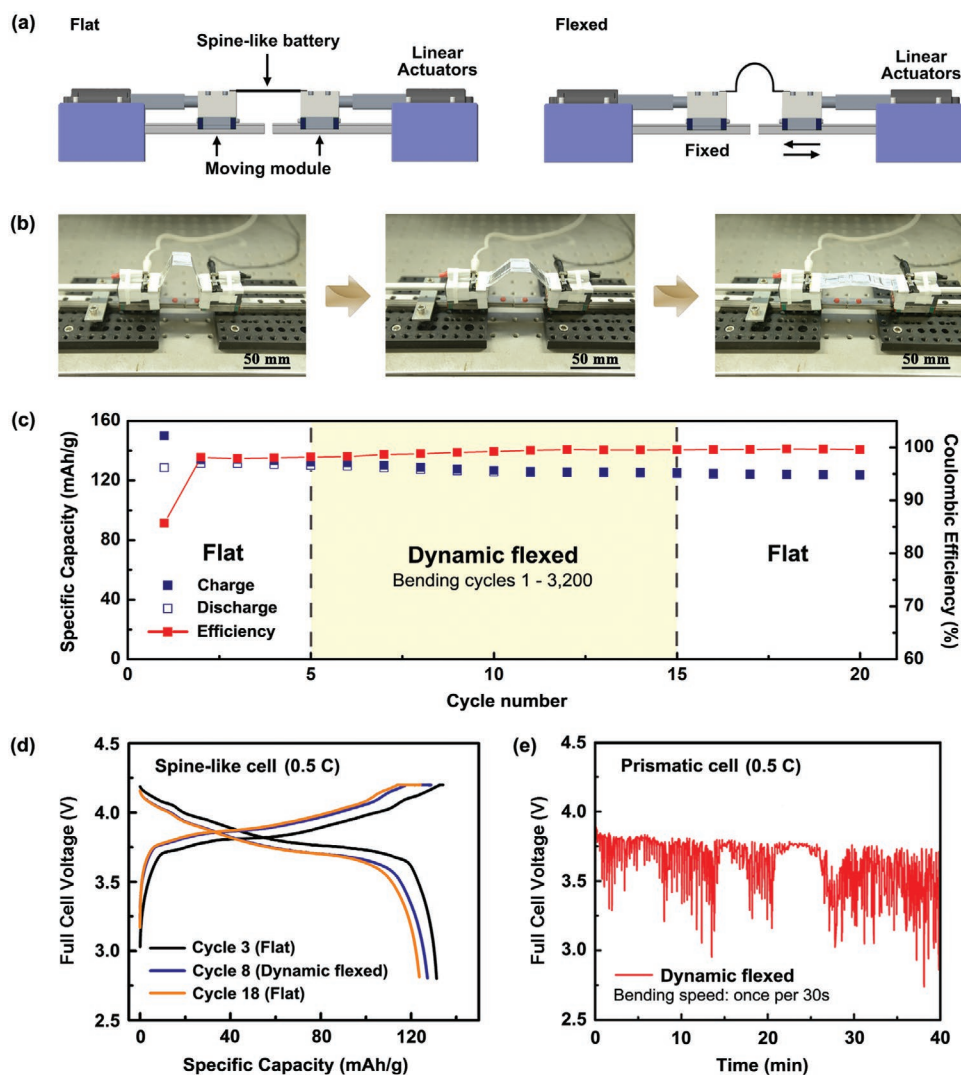


Figure 3. The dynamic mechanical load test. a) The schematic of the custom-made flexing apparatus. b) Optical images of the battery in the different state during the dynamic mechanical load test. c) The cycling performance of a spine-like battery in different configurations under repetitive mechanical load test. d) Galvanostatic charge–discharge curves for 3rd, 8th, and 18th cycles of the spine-like cell. e) The voltage profile of the prismatic cell under flexed condition at discharge rate of 0.5 C. The battery dimensions are the same with spine-like cell.

wrapped on a human wrist by finite element simulations. It is evident in Figure 5c that the maximum strain of spine-like structure is only 0.08%, negligible compared with those in prismatic (1.8%) and stacked (1.1%) structures. For comparison, the yield strain of Al foils and Cu foils are 0.47% and 0.73%, respectively (Figure S9, Supporting Information). Therefore, our design is well within the elastic regime of metal substrates, while conventional designs approach or go beyond the elastic limit of Al. Such results echo well with both optical and scanning electron microscopy (SEM) images in Figures S4 and S8 (Supporting Information) that cracks occur in the two conventional designs but not our spine-like battery subjected to bending cycles. In the spine-like design, the strain concentrates at the boundary of marrow and vertebra (see Figure S10 in the Supporting Information). Similarly, torsion up to 90° only results in maximum strain of 0.04%, which occurs in the thin marrow part shown in Figure 5d. Besides the robustness

of bending and torsion in the spine-like battery, the Young's modulus and the tensile strength are also important for practical application. The stress–strain response of the spine-like cell is shown in Figure S11 (Supporting Information), which illustrates the tensile strength of 80 and 115 Mpa, respectively, consistent with results in bare aluminum and copper foil (Figure S8, Supporting Information). Simulations and experiments above demonstrate that the rational design of spine-like structure is critical to the high flexibility of our cells, and it is well suitable for flexible devices (see the Supporting Information for more details).

In summary, we have demonstrated a facile and scalable method to fabricate spine-like Li-ion batteries with remarkable flexibility, mechanical stability, and electrochemical performance. The as-designed structure shows excellent stability upon flat, flexed, and twisted configuration. Moreover, the energy density can be over 85% of conventional prismatic or stack

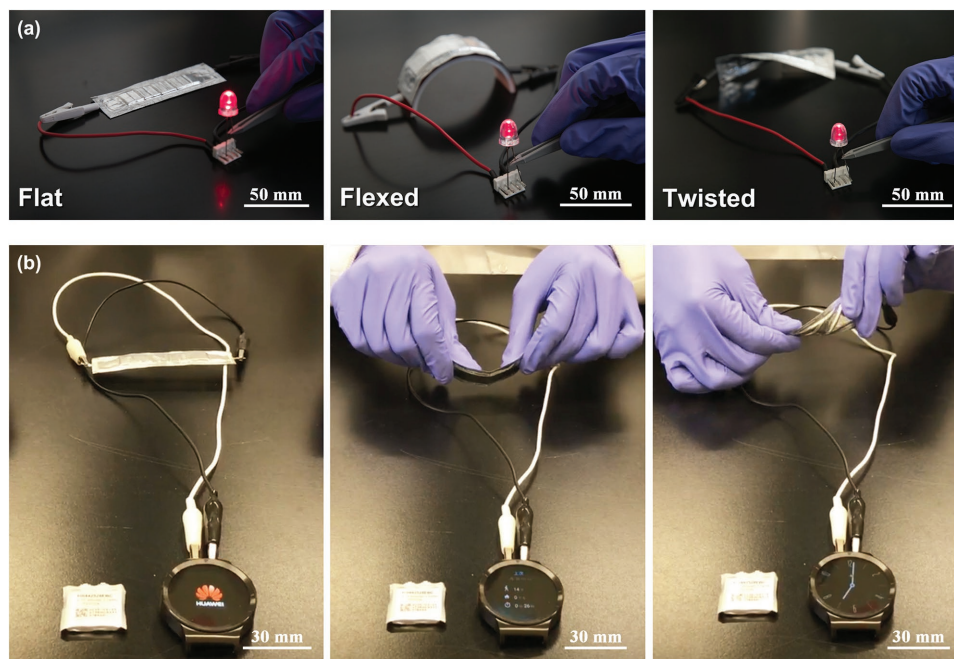


Figure 4. The applications of spine-like batteries to charge LED and smart watch. a) Powering an LED diode. b) Powering a smart watch with the battery in flat, flexed, and twisted configurations. The different content on the screen in three states is due to the continuous operation of the smart watch accompanied with continuous deformation of the battery. The original battery (weight: 5.27 g, capacity: 300 mA h) is put on the left of the panel.

pouch cells. A capacity retention over 94.3% after 100 cycles is achieved at 0.2 C even with flexing to a diameter of 20 mm and twisting angle to 90°. The cell also remained stable power

output and cycling performance during continuous dynamic mechanical load tests. Numerical simulation results confirm that the spine-like structure sustained smaller strain ($\approx 0.08\%$) com-

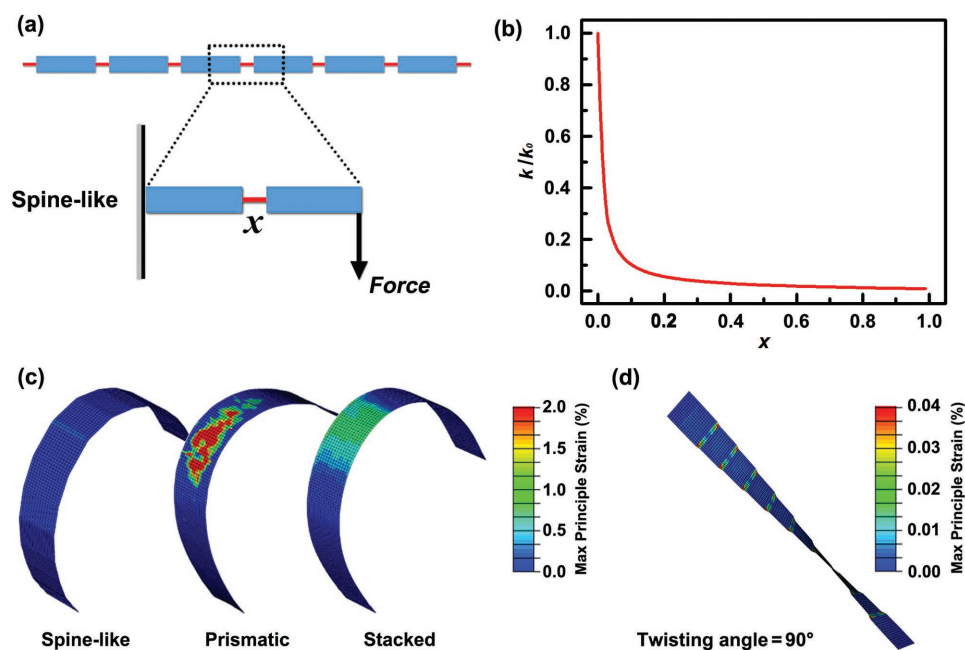


Figure 5. Simulation results of the spine-like battery. a) Schematic of the spine-like design. The thick stacks and soft interconnects are marked in blue and red, respectively. The dashed box highlights the structural element with the length fraction of soft interconnect x . b) The relative effective bending stiffness k/k_0 as a function of the fraction x ; k_0 represents the bending stiffness for the structure with only thick stacks. c) Finite element results of the maximum principle strain of the spine-like, prismatic, and stacked structures subjected to bend on a cylinder with elliptical cross-section ($a = 3.2$ cm, $b = 1.8$ cm), similar to the geometry of human wrist. d) Finite element results of the maximum principle strain of the spine-like structure subjected to torsion with twisting angle of 90°.

pared with prismatic cell (1.8%). The excellent electrochemical and mechanical properties of our design are promising for wide applications in flexible and wearable electronics.

Experimental Section

Battery Fabrication: Commercially obtained LiCoO₂ (MTI Corp.) and graphite (MTI Corp.) were utilized as cathode and anode materials. The LCO and graphite electrodes were prepared by coating slurries that mixed active electrodes with carbon black (Timcal Super C45) and polyvinylidene fluoride (PVDF) (Kynar HSV900) (8:1:1 wt/wt/wt) on the aluminum and copper foil, respectively. The electrodes were then dried in a vacuum oven at 120 °C for 8 h. After drying, the electrodes and separator (Celgard 2500) were cut into the designed geometry. A piece of polyethylene foil (65 μm) was placed on top of the backbone part, to reduce stress at the folding edge. Then, the electrodes were assembled in the aluminized polyethylene (Sigma-Aldrich) package in an argon-filled glovebox (O₂ < 0.1 ppm, H₂O < 0.1 ppm) using 1 M LiPF₆ in the ethylene carbonate/diethyl carbonate (1:1 vol/vol) (BASF Corp.) as electrolyte. Then a customized high-temperature vacuum sealer was used to seal the aluminized polyethylene packaging material. This sealer offers a strong vacuum environment and good internal pressure to the components of the pouch. The length of the obtained 0623 spine-like cell was 69 mm and the length of each hard component was 5 mm, the interconnected space between hard components was 1 mm (more details in Figure S1 in the Supporting Information).

Electrochemical Tests: The spine-like LiCoO₂/graphite batteries were subjected to charging to 4.2 V first and potentiostatic hold at 4.2 V was added until the current density decreased to 0.05 C to ensure the full charge of LCO, the cut off voltage of discharge was 2.8 V. Full cells were tested using the battery analyzers of Landt Instruments (Model: CT 2001) and the Bio-logic SAS (Model: VMP3).

Characterization: The morphology of the electrodes was observed with an SEM (ZEISS Sigma VP). Mechanical strain stress curve was conducted along the in-plane direction with a model 5948 MicroTester Instron instrument.

Simulation: The bending and twisting deformation of the spine-like battery, prismatic and stacked battery, were simulated using 3D nonlinear finite element method, implemented in the commercial software ABAQUS. In all cases, four-node quadrilateral stress/displacement shell elements (S4R) with reduced integration were used and the mesh density was verified by mesh convergence studies. For simplicity, linear isotropic elasticity was adopted for the battery structure with the effective modulus and Poisson ratio-based experimental parameters. The simply supported boundaries were adopted at the ends of structures and the cylinder was fixed.

Supporting Information

Supporting Information is available from the Wiley Online Library or from the author.

Acknowledgements

G.Y.Q. and B.Z. contributed equally to this work. Y.Y. acknowledges support from startup funding by Columbia University. This work is supported by the NSFMRSEC program through Columbia in the Center for Precision Assembly of Superstratic and Superatomic Solids (DMR-1420634) and sponsored by the China Scholarship Council (CSC) graduate scholarship. The photography and camera services are offered by Teng Yang NYC Media Studio and Jane Nisselson from Columbia Engineering. The authors would like to acknowledge support from Prof. Kristin Myers, Prof. Arvind Narayanaswamy and Dr. Charles Jayyosi

of Department of Mechanical Engineering at Columbia University on mechanical measurement.

Note: The y axis labels in Figure 2c,e and in 3d,e were corrected to read "Full Cell Voltage (V)", i.e., for half cells, on March 19, 2018, after initial publication online. The supporting information was also corrected.

Conflict of Interest

The authors declare no conflict of interest.

Keywords

energy density, flexible batteries, lithium-ion batteries

Received: August 29, 2017

Revised: December 10, 2017

Published online: January 31, 2018

- [1] J. A. Rogers, Z. Bao, K. Baldwin, A. Dodabalapur, B. Crone, V. R. Raju, V. Kuck, H. Katz, K. Amundson, J. Ewing, P. Drzaic, *Proc. Natl. Acad. Sci. USA* **2001**, *98*, 4835.
- [2] L. Nyholm, G. Nystrom, A. Mihranyan, M. Stromme, *Adv. Mater.* **2011**, *23*, 3751.
- [3] W. Liu, M. S. Song, B. Kong, Y. Cui, *Adv. Mater.* **2017**, *29*, 1603436.
- [4] Y. Khan, A. E. Ostfeld, C. M. Lochner, A. Pierre, A. C. Arias, *Adv. Mater.* **2016**, *28*, 4373.
- [5] Y. H. Jung, T. H. Chang, H. Zhang, C. Yao, Q. Zheng, V. W. Yang, H. Mi, M. Kim, S. J. Cho, D. W. Park, H. Jiang, J. Lee, Y. Qiu, W. Zhou, Z. Cai, S. Gong, Z. Ma, *Nat. Commun.* **2015**, *6*, 7170.
- [6] Y. Chen, J. Au, P. Kazlas, A. Ritenour, H. Gates, M. McCreary, *Nature* **2003**, *422*, 6936.
- [7] D. H. Kim, N. Lu, R. Ma, Y.-S. Kim, R. H. Kim, S. Wang, J. Wu, S. M. Won, H. Tao, A. Islam, K. J. Yu, T. I. Kim, R. Chowdhury, M. Ying, L. Xu, M. Li, H. J. Chung, H. Keum, M. McCormick, P. Liu, Y. W. Zhang, F. G. Omenetto, Y. Huang, T. Coleman, J. A. Roger, *Science* **2011**, *333*, 838.
- [8] S. C. Mannsfeld, B. C. Tee, R. M. Stoltenberg, C. V. Chen, S. Barman, B. V. Mui, A. N. Sokolov, C. Reese, Z. Bao, *Nat. Mater.* **2010**, *9*, 859.
- [9] Y. Sun, J. A. Rogers, *Adv. Mater.* **2007**, *19*, 1897.
- [10] G. Schwartz, B. C. Tee, J. Mei, A. L. Appleton, D. H. Kim, H. Wang, Z. Bao, *Nat. Commun.* **2013**, *4*, 1859.
- [11] Z. Wang, Z. Wu, N. Bramnik, S. Mitra, *Adv. Mater.* **2014**, *26*, 970.
- [12] M. H. Park, K. Kim, J. Kim, J. Cho, *Adv. Mater.* **2010**, *22*, 415.
- [13] H. Liu, T. Zhao, W. Jiang, R. Jia, D. Niu, G. Qiu, L. Fan, X. Li, W. Liu, B. Chen, Y. Shi, L. Yin, B. Lu, *Adv. Funct. Mater.* **2015**, *25*, 7071.
- [14] H. Gwon, H.-S. Kim, K. U. Lee, D.-H. Seo, Y. C. Park, Y.-S. Lee, B. T. Ahn, K. Kang, *Energy Environ. Sci.* **2011**, *4*, 1277.
- [15] A. M. Gaikwad, G. L. Whiting, D. A. Steingart, A. C. Arias, *Adv. Mater.* **2011**, *23*, 3251.
- [16] A. M. Gaikwad, H. N. Chu, R. Qeraj, A. M. Zamarayeva, D. A. Steingart, *Energy Technol.* **2013**, *1*, 177.
- [17] N. Li, Z. Chen, W. Ren, F. Li, H. M. Cheng, *Proc. Natl. Acad. Sci. USA* **2012**, *109*, 17360.
- [18] Z. Pan, J. Ren, G. Guan, X. Fang, B. Wang, S.-G. Doo, I. H. Son, X. Huang, H. Peng, *Adv. Energy Mater.* **2016**, *6*, 1600271.
- [19] W. Weng, Q. Sun, Y. Zhang, S. He, Q. Wu, J. Deng, X. Fang, G. Guan, J. Ren, H. Peng, *Adv. Mater.* **2015**, *27*, 1363.
- [20] Z. Zhang, L. Wang, Y. Li, Y. Wang, J. Zhang, G. Guan, Z. Pan, G. Zheng, H. Peng, *Adv. Energy Mater.* **2017**, *7*, 1601814.
- [21] H. Lin, W. Weng, J. Ren, L. Qiu, Z. Zhang, P. Chen, X. Chen, J. Deng, Y. Wang, H. Peng, *Adv. Mater.* **2014**, *26*, 1217.

- [22] B. Liu, J. Zhang, X. Wang, G. Chen, D. Chen, C. Zhou, G. Shen, *Nano Lett.* **2012**, *12*, 3005.
- [23] D.-W. Wang, I. Gentle, F. Li, J. Zhao, G. Q. Lu, H.-M. Cheng, W. Ren, Z.-G. Chen, J. Tan, Z.-S. Wu, *ACS Nano* **2009**, *3*, 1745.
- [24] Y. Gogotsi, P. Simon, *Science* **2011**, *334*, 917.
- [25] Q. Cheng, Z. Song, T. Ma, B. B. Smith, R. Tang, H. Yu, H. Jiang, C. K. Chan, *Nano Lett.* **2013**, *13*, 4969.
- [26] A. M. Zamarayeva, A. E. Ostfeld, M. Wang, J. K. Doney, I. Deckman, B. P. Lechêne, G. Davies, D. A. Steingart, A. C. Arias, *Sci. Adv.* **2017**, *3*, e1602051.
- [27] L. Hu, H. Wu, Y. Y. Fabio La Mantia, Y. Cui, *ACS Nano* **2010**, *4*, 5843.
- [28] M. Koo, K. I. Park, S. H. Lee, M. Suh, D. Y. Jeon, J. W. Choi, K. Kang, K. J. Lee, *Nano Lett.* **2012**, *12*, 4810.
- [29] J. Ren, L. Li, C. Chen, X. Chen, Z. Cai, L. Qiu, Y. Wang, X. Zhu, H. Peng, *Adv. Mater.* **2013**, *25*, 1155.
- [30] J. Ren, Y. Zhang, W. Bai, X. Chen, Z. Zhang, X. Fang, W. Weng, Y. Wang, H. Peng, *Angew. Chem., Int. Ed. Engl.* **2014**, *53*, 7864.
- [31] S. Xu, Y. Zhang, J. Cho, J. Lee, X. Huang, L. Jia, J. A. Fan, Y. Su, J. Su, H. Zhang, H. Cheng, B. Lu, C. Yu, C. Chuang, T. I. Kim, T. Song, K. Shigeta, S. Kang, C. Dagdeviren, I. Petrov, P. V. Braun, Y. Huang, U. Paik, J. A. Rogers, *Nat. Commun.* **2013**, *4*, 1543.
- [32] Z. Song, T. Ma, R. Tang, Q. Cheng, X. Wang, D. Krishnaraju, R. Panat, C. K. Chan, H. Yu, H. Jiang, *Nat. Commun.* **2014**, *5*, 3140.
- [33] L. Hu, J. W. Choi, Y. Yang, S. Jeong, F. La Mantia, L. F. Cui, Y. Cui, *Proc. Natl. Acad. Sci. USA* **2009**, *106*, 21490.